41522: Advanced Dynamics & Vibrations Course Exercise

Sebastian Mostek

May 2025

Abstract

This paper examines the dynamics of a clamped-clamped Euler beam subject to pretensioning, viscous damping, and a point mass at its center. The purpose is to provide a theoretical understanding for the seemingly anomamous frequency response of the NoDyBeam nonlinearity inducer. Ultimately it will be shown that the behavior is well-modeled by a second-order harmonically forced ODE with nonlinear damping and restoring forces.

1 Equation of Motion

Our model is a 1D beam of length l with non-uniform mass density $\lambda(X)$ and rotational inertia density $j(X)$, subject to a force per unit length $f(X)$ as well as a uniform harmonic forcing $U_0(\tilde{t}) = ql\sin(\tilde{\Omega}\tilde{t})$. By applying force and moment balance to a differential beam segment, shown in Fig. (1), we see

$$\begin{aligned} N' &= 0 \\ V' &= f - \lambda a \\ M' - U'N - V &= j\ddot{\theta} \end{aligned} \tag{1}$$

where θ is the angular displacement of the beam segment and $\ddot{\theta}$ is its angular acceleration; a is the inertial acceleration of the beam, equal to $\ddot{U} + \ddot{U}_0$. We further assume that the beam segment cannot move in the X-direction.

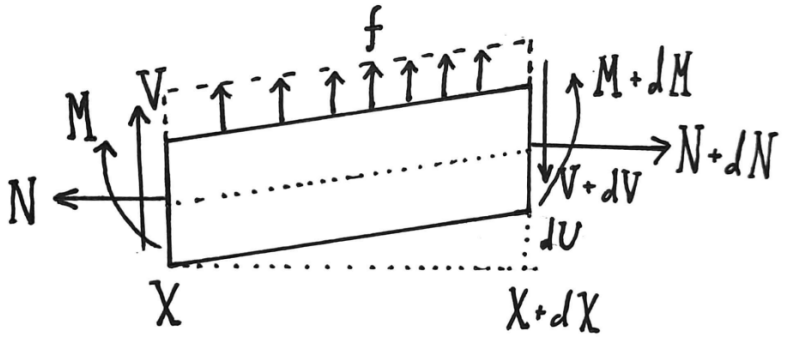

Figure 1: Differential beam segment subject to tensile and shear and external forces N, V, and f, as well as a moment M. The segment's mass is λdX and its rotational inertia (relative to rotations in the plane of the page) is $j\,dX$. If I knew of a better way to draw this than by hand, I would have done so.

When θ is small, the beam's slope $U' = \tan\theta \approx \theta$. Under the same assumption, Hooke's Law of Beam Bending becomes $M = EIU''$, where E and I are the beam's Elastic Modulus and Second

Moment of Area, both taken to be uniform. Inserting these changes into (1), then differentiating the third equation gives

$$EIU'''' - U''N - f + \lambda a = (j\ddot{U}')' \tag{2}$$

The tension force N is uniform and is given by

$$N(l,\tilde{t}) = EA\left(\alpha + \frac{1}{2l}\int_0^l (U')^2 dX\right) \tag{3}$$

where A is the cross-sectional area of the beam and α is the proportional pretensioning of the beam; $\alpha = 0$ corresponds to no tension, while positive and negative α correspond to tension and compression, respectively. Meanwhile, we model the proof mass as a point particle, so a Dirac Delta Function is used to incorporate its effects into the otherwise continuous system. For instance, the mass density function λ is given by $\rho A + M\delta(X - \frac{l}{2})$. Inserting all this into (2) gives

$$\begin{aligned} EIU'''' - EAU''\left(\alpha + \frac{1}{2l}\int_0^l (U')^2 dX\right) + \left(C_b\dot{U} + (C_{M1}\dot{U} + C_{M2}\dot{U}^2)\delta(X - \tfrac{l}{2})\right) \\ + (\rho A + M\delta(X - \tfrac{l}{2}))(\ddot{U} - ql\tilde{\Omega}^2\sin(\tilde{\Omega}\tilde{t}) = \left(J\delta(X - \tfrac{l}{2})\ddot{U}'\right)' \end{aligned} \tag{4}$$

To reduce the total number of parameters, we introduce nondimensional variables $x = X/l$, $t = \omega_0\tilde{t}$, and $u = U/l$, where $\omega_0^2 = EI/(\rho A l^4)$ is the natural frequency of an undamped Euler beam. The chain rule is necessary to adjust the many derivatives:

$$\begin{aligned} U' &= \frac{\partial U}{\partial X} = \frac{\partial(lu)}{\partial x}\frac{\partial x}{\partial X} = \frac{\partial u}{\partial x} \\ \dot{U} &= \frac{\partial U}{\partial \tilde{t}} = \frac{\partial(lu)}{\partial t}\frac{\partial t}{\partial \tilde{t}} = \omega_0 l\frac{\partial u}{\partial t} \end{aligned} \tag{5}$$

Making these changes to (4) (and multiplying everything by $l^3/EI = 1/\omega_0^2\rho A l$) yields a more manageable nondimensionalized equation of motion:

$$\begin{aligned} u'''' - u''s^2\left(\alpha + \tfrac{1}{2}\int_0^1 (u')^2 dx\right) + c_b\dot{u} + (c_{m1}\dot{u} + c_{m2}\dot{u}^2)\delta(x - \tfrac{1}{2}) + \\ \left(1 + m\delta(x - \tfrac{1}{2})\right)\left(\ddot{u} - q\Omega^2\sin(\Omega t)\right) = \left(\mu m\delta(x - \tfrac{1}{2})\ddot{u}'\right)' \end{aligned} \tag{6}$$

where now the primes and overdots refer to derivatives with respect to x and t, and the new constants are defined as

$$\begin{aligned} s^2 &= \tfrac{l^2 A}{I} & c_b &= \tfrac{1}{\rho A\omega_0}C_b \\ m &= \tfrac{M}{\rho A l} & c_{m1} &= \tfrac{1}{\rho A l\omega_0}C_{M1} \\ \Omega &= \tfrac{\tilde{\Omega}}{\omega_0} & c_{m2} &= \tfrac{1}{\rho A}C_{M2} \\ & & \mu &= \tfrac{J}{Ml^2} \end{aligned} \tag{7}$$

Each of these nondimensional parameters can be interpreted as ratios of physical quantities: m is the ratio of the mass of the point to the mass of the beam; μ is the ratio of the mass' rotational inertia to that of a point of equal mass at distance l; Ω is the ratio of the driving frequency to the natural frequency. s is a geometric ratio relating the beam's length to its cross-section; in the case of a rectangular beam of thickness h, $s = \sqrt{12}\cdot l/h$. The damping terms are more difficult to interpret as C_b, C_{M1}, and C_{M2} each have distinct units that are difficult to intuitively grasp on their own. C_b, for instance, has units of force per length per velocity, or equivalently, mass per length per time, but generally I find it is instructive to think of these values as ratios of the power per unit being dissipated by the damping relative to the kinetic energy per unit length.

Nonlinearities in this equation are the quadratic damping term $c_{m2}\dot{u}^2$ and the integral tension term.

2 Eigenvalue Problem

2.1 Linearized System

Ignoring the damping, nonlinearities, and forcing in (6) gives

$$u'''' - u''s^2\alpha + (1 + m\delta(x - \tfrac{1}{2}))\ddot{u} = \left(\mu m\delta(x - \tfrac{1}{2})\ddot{u}'\right)' \tag{8}$$

Assuming a harmonic solution of the form $u(x,t) = \phi(x)\sin(\omega t)$, this PDE becomes an ODE for ϕ:

$$\phi'''' - s^2\alpha\phi'' - \omega^2\left(1 + m\delta(x - \tfrac{1}{2})\right) = -\omega^2\left(\mu m\delta(x - \tfrac{1}{2})\phi'\right)' \tag{9}$$

Converting this into EVP form, $K\phi = \lambda L\phi$, we see that

$$\begin{aligned} \lambda &= \omega^2 \\ K &= -s^2\alpha\frac{d^2}{dx^2} + \frac{d^4}{dx^4} \\ L &= \left(1 + m\delta(x - \tfrac{1}{2})\right) - \frac{d}{dx}\left(\mu m\delta(x - \tfrac{1}{2})\frac{d}{dx}\right) \end{aligned} \tag{10}$$

with boundary conditions given by

$$\begin{aligned} \phi(0) = \phi(1) = 0 \\ \phi'(0) = \phi'(1) = 0 \end{aligned} \tag{11}$$

Solving this EVP requires identifying the eigenfuctions ϕ_i and their corresponding eigenvalues λ_i, thereby identifying the principal mode shapes and frequencies of the beam.

2.2 EVP Properties

The delta functions make (9) not directly solvable, but it is still possible to infer information about the solution from the structure of the problem.

One useful property is self-adjointness: an EVP is self-adjoint if, for any functions u and v satisfying the boundary conditions,

$$\int_0^1 (uKv - vKu)dx = \int_0^1 (uLv - vLu)dx = 0 \tag{12}$$

Proving this relation in depth is not necessary nor informative, so suffice to say that through integration by parts the higher-order derivatives can be reduced and canceled out. For instance, the K integral can be reduced to

$$\begin{aligned} -s^2\alpha\left([uv' - vu']_0^1 - \int_0^1 (u'v' - v'u')dx\right) + \\ \left([uv''' - vu''']_0^1 - [u'v'' - v'u'']_0^1 + \int_0^1 (u''v'' - v''u'')dx\right) \end{aligned} \tag{13}$$

For which every term cancels out to zero so long as u and v satisfy the boundary conditions given in (11). A similar procedure shows that the L integral also reduces to 0, making the EVP self-adjoint.

Second, an EVP is completely definite if, for any function u satisfying the boundary conditions,

$$\int_0^1 uKu\,dx > 0 \ \wedge \ \int_0^1 uLu\,dx > 0 \tag{14}$$

or if both integrals are < 0. Again ignoring unnecessary steps, it can be shown that

$$\begin{aligned} \int_0^1 uKu\,dx &= s^2\alpha\int_0^1 (u')^2dx + \int_0^1 (u'')^2dx \\ \int_0^1 uLu\,dx &= \int_0^1 u^2dx + mu(\tfrac{1}{2})^2 + \mu mu'(\tfrac{1}{2})^2 \end{aligned} \tag{15}$$

The second integral is always > 0 since μ and m are both positive, but the first equation could be negative if α is made sufficiently negative, specifically if

$$\alpha > -\frac{\int_0^1 (u'')^2 dx}{\int_0^1 (su')^2 dx} \tag{16}$$

which is to say that the beam will behave normally so long as it is not compressed below a certain threshold. While this condition remains somewhat unhelpful because u is an unspecified function, if we were able to determine the eigenfunctions of (9), we could use (16) to identify the buckling load of the beam.

The practical effect of evaluating these properties is that, despite not knowing anything of the shapes of the solutions, we can infer useful information about them. For instance, any EVP that is both self-adjoint and completely definite has only real, positive eigenvalues. For (9), so long as (16) holds, this means that (because $\lambda_i = \omega_i^2$) all of the system's modes are associated with real-valued frequencies. When the condition on α is not met, the EVP becomes *semidefinite* and it becomes possible for its eigenvalues to be negative, implying complex ω_i, a situation discussed in greater detail later on.

2.3 Rayleigh Quotient

Another useful property of self-adjoint and completely definite EVPs is related to its Rayleigh Quotient, a functional defined as

$$R[u] = \frac{\int_0^1 uKu\, dx}{\int_0^1 uLu\, dx} \tag{17}$$

For such EVPs, this ratio is minimized when $u = \phi_1$, the lowest mode shape. Moreover, $R[\phi_1] = \lambda_1$, meaning that the lowest value of the Rayleigh Quotient that we can find can be used to approximate the system's lowest natural frequency.

For our EVP, we can use the formulae from (15) to write the Quotient as

$$R[u] = \frac{s^2\alpha \int_0^1 (u')^2 dx + \int_0^1 (u'')^2 dx}{\int_0^1 u^2 dx + mu(\frac{1}{2})^2 + \mu m u'(\frac{1}{2})^2} \tag{18}$$

Testing this tool out on a simple example function $\phi(x) = x^2(1-x)^2$, we have

$$R = \frac{s^2\alpha \cdot 0.01905 + 0.8}{0.00159 + m \cdot 0.00391} \tag{19}$$

where the individual derivatives and integrals were computed numerically using software.

Meanwhile, if we assume a more complicated mode shape equal to that of a clamped-clamped beam *without* a point mass: $\phi(x) = J(\lambda_1 \frac{x}{l}) - \frac{J(\lambda_1)}{H(\lambda_1)} H(\lambda_1 \frac{x}{l})$, where $J(v) = \cosh v - \cos v$, $H(v) = \sinh v - \sin v$, $\lambda_1 = 4.7300$, and $l = 1$. Evaluating the Rayleigh Quotient on this equation gives

$$R = \frac{s^2\alpha \cdot 12.303 + 500.534}{1 + m \cdot 2.522} \tag{20}$$

For a representative example beam with the following properties

$$\begin{aligned} &b \times h \times l = 10 \times 0.15 \times 120\,\mathrm{mm}^3 \\ &M = 25\,\mathrm{g} \\ &E = 206\,\mathrm{GPa} \\ &\rho = 7850\,\mathrm{kg/m}^3 \end{aligned} \tag{21}$$

we have $s = 2\sqrt{3}\frac{l}{h} = 2771.281$, and $m = M/(\rho A l) = 17.693$. Values of the Rayleigh Quotient for both example functions at various values of α are summaried in Table (1).

Recalling that the minimum possible value of R is the lowest eigenvalue of the EVP, and that $\lambda = \omega^2$, it follows that the lower value in each row corresponds to an estimate for the natural

	$\phi = x^2(1-x)^2$	$\phi = J(v) - kH(v)$
$\alpha = 0$	11.315	10.971
$\alpha = 1.808 \cdot 10^{-5}$	48.732	48.424
$\alpha = 8.33 \cdot 10^{-4}$	1735.569	1736.899

Table 1: Estimates of the eigenvalues of (9) using (19) and (20) at varying values of α.

frequency of the system. To determine the value of these natural frequencies, we must undo the layers of nondimensionalization: $u(x,t) = \phi(x)\sin(\omega t)$, and $t = \omega_0 \tilde{t}$, with $\omega_0^2 = EI/(\rho A l^4)$. Thus the true natural frequency is

$$\tilde{\omega}_1 = \omega_1 \omega_0 = \sqrt{\lambda_1 \frac{EI}{\rho A l^4}} \tag{22}$$

Using the lowest calculated value of the Rayleigh Quotient in each loading as an estimate for λ_1, we have

$$\begin{aligned} \alpha = 0: &\quad \tilde{\omega}_1 \approx 8.1\,\text{Hz} \\ \alpha = 1.808 \cdot 10^{-5}: &\quad \tilde{\omega}_1 \approx 17.1\,\text{Hz} \\ \alpha = 8.33 \cdot 10^{-4}: &\quad \tilde{\omega}_1 \approx 102.1\,\text{Hz} \end{aligned} \tag{23}$$

The utility of these predictions is difficult to determine, but is generally dubious. These values are necessarily overestimates given how the Rayleigh Quotient works, but then again the effect of viscous damping (which we ignored) would be to reduce the response frequency. Although the presence of delta functions in L makes it slightly impractical, I attempted to plot $K\phi - \lambda_1 L\phi$ to test the quality of the assumed mode shape. Even for $\alpha = 0$, the graph is not near 0 for either solution model, and the predictions only get worse as tension is added. It is clear that the effect of the mass on the mode-shape is significant yet very difficult to accurately account for, at least for m as large as it is (the point mass over 17 times as heavy as the beam).

We are given a graph of the NoDyBeam free-response which reveals a natural frequency on the order of 17 Hz, but without knowing the values of the parameters for that test, we cannot use that to judge the quality of the frequency predictions.

3 Discrete Models: Mode Shape Expansion

3.1 EOM to coupled ODEs

Turning to a different solution method, let us construct a solution of the form

$$u(x,t) = \sum_j \phi_j(x) y_j(t) \tag{24}$$

where we assume the spatial terms ϕ_j to be the modes of a standard clamped-clamped beam:

$$\phi_j(x) = J(\lambda_j \tfrac{x}{l}) - \frac{J(\lambda_j)}{H(\lambda_j)} H(\lambda_j \tfrac{x}{l}) \tag{25}$$

with the same definitions for J and H as given in the previous section.

To improve the readability of the following equations, I have chosen to represent the many linear combinations using Implicit Summation Notation, making $u = \phi_j y^j$. It isn't a perfect solution, it makes exponents slightly more inconvenient for example, but I consider it worthwhile.

The goal is to utilize the orthogonality of modes to break our one large EOM into smaller, distinct equations for each of the y^j's. For instance, since $\int_0^1 \phi_i \phi_j dx = \delta^i_j$, it follows that $\int_0^1 \phi_i u dx =$

y^i. Other useful orthogonality relations are summarized:

$$\begin{gathered}\int_0^1 \phi_i'\phi_j' dx = -\int_0^1 \phi_i\phi_j'' dx = r_j^1\delta_j^i \\ \int_0^1 \phi_i\phi_j'''' dx = \int_0^1 \phi_i''\phi_j'' dx = r_j^2\delta_j^i \\ \int_0^1 \phi_j dx = r_j^3 \qquad \phi_j(\tfrac{1}{2}) = r_j^4 \qquad \phi_j'(\tfrac{1}{2}) = r_j^5 \\ \mathbf{r} = \begin{bmatrix} 12.30 & 46.05 \\ 500.5 & 3804 \\ 0.8309 & 0 \\ 1.588 & 0 \\ 0 & -11.42 \end{bmatrix}\end{gathered} \tag{26}$$

The $\mathbf{r}$ matrix could, in principle, extend for infinite columns, but for practicality's sake we will only be using a two-mode approximation, so the information given is all we'll need.

Plugging (24) into (6) and taking the inner product of the whole thing, we get the rather daunting equation

$$\begin{aligned}&\int_0^1 \phi_i\phi_j''''dx\, y^j - s^2\alpha\int_0^1 \phi_i\phi_j''dx\, y^j - \tfrac{1}{2}s^2\int_0^1 \phi_i\left(\int_0^1 (\phi_j' y^j)^2 dx\right)\phi_j''dx\, y^j \\ &\quad + c_b\int_0^1 \phi_i\phi_j dx\, \dot{y}^j + c_{m1}\int_0^1 \phi_i\phi_j\delta dx\, \dot{y}^j + c_{m2}\int_0^1 \phi_i(\phi_j\dot{y}^j)^2\delta dx \\ &+ \int_0^1 \phi_i(1+m\delta)(\phi_j\ddot{y}^j - q\Omega^2\sin\Omega t)dx - \int_0^1 \phi_i(\mu m\delta\phi_j'\ddot{y}^j)'dx = 0\end{aligned} \tag{27}$$

where δ is a abbreviation of $\delta(x-\frac{1}{2})$. Most of these integrals can be resolved readily using (26), and the lattermost only requires integration by parts to simplify. However, the two integrals containing squared quantities deserve special attention. Recalling that we are using a two-mode expansion for u, the first difficult integral, with the factor of $\frac{1}{2}s^2$, can be broken down as follows:

$$\begin{aligned}\int_0^1 (\phi_j' y^j)^2 dx &= \int_0^1 (\phi_1')^2 dx\, y_1^2 + 2\int_0^1 \phi_1\phi_2 dx\, y_1 y_2 + \int_0^1 (\phi_2')^2 dx\, y_2^2 = r_{11}y_1^2 + r_{12}y_2^2 \\ \int_0^1 \phi_i(r_{11}y_1^2 + r_{12}y_2^2)\phi_j''dx\, y^j &= -(r_{11}y_1^2 + r_{12}y_2^2)r_j^1\delta_j^i y^i = -(r_{11}y_1^2 + r_{12}y_2^2)r_i^1 y^i\end{aligned} \tag{28}$$

Similarly, the other difficult integral, with the factor of c_{m2}, can be resolved by expanding out the implicit sum:

$$\int_0^1 \phi_i(\phi_j\dot{y}^j)^2\delta dx = \phi_i(\tfrac{1}{2})\left(\phi_1(\tfrac{1}{2})\dot{y}_1 + \phi_2(\tfrac{1}{2})\dot{y}_2\right)^2 = r_i^4(r_1^4\dot{y}_1)^2 \tag{29}$$

The effect of these many integrals is to convert (27) into an equation for y^i. In order for the equation to hold in general, it must hold separately for each value of i. For $i = 1$ we have

$$\begin{aligned}(r_{21} + s^2\alpha r_{11})y_1 + \tfrac{1}{2}s^2(r_{11}y_1^2 + r_{12}y_2^2)r_{11}y_1 + (c_b + c_{m1}r_{41}^2)\dot{y}_1 + c_{m2}r_{41}^3\dot{y}_1^2 \\ + \ddot{y}_1(1 + mr_{41}^2) - (r_{31} + r_{41}m)q\Omega^2\sin\Omega t = 0\end{aligned} \tag{30}$$

whereas for $i = 2$ we have

$$(r_{22} + s^2\alpha r_{12})y_2 + \tfrac{1}{2}s^2(r_{11}y_1^2 + r_{12}y_2^2)r_{12}y_2 + c_b\dot{y}_1 + \ddot{y}_2(1 + \mu m r_{52}^2) = 0 \tag{31}$$

3.2 Ziegler Classification

Ignoring nonlinear terms (the $\frac{1}{2}s^2$ and c_{m2} terms), we can rewrite (30) and (31) in matrix form:

$$\begin{aligned}&\begin{bmatrix} 1 + mr_{41}^2 & 0 \\ 0 & 1 + \mu m r_{52}^2 \end{bmatrix}\ddot{\mathbf{y}} + \begin{bmatrix} c_b + r_{41}^2 c_{m1} & 0 \\ 0 & c_b \end{bmatrix}\dot{\mathbf{y}} + \\ &\begin{bmatrix} r_{21} + r_{11}s^2\alpha & 0 \\ 0 & r_{22} + r_{12}s^2\alpha \end{bmatrix}\mathbf{y} = \begin{bmatrix} (r_{31} + r_{41}m)q\Omega^2\sin\Omega t \\ 0 \end{bmatrix}\end{aligned} \tag{32}$$

where $\mathbf{y} = [y_1\ y_2]^T$.

That all of these matrices are symmetric means that this system is *completely dissipative*: it has non-circulatory forces from the stiffness matrix, K, and its only nonconservative forces are the dissipative forces in the positive definite damping matrix. This means that, ignoring forcing ($q = 0$), $\mathbf{y} = \mathbf{0}$ is a stable equilibrium so long as the stiffness matrix is positive definite ($\mathbf{y}^T K\mathbf{y} > 0$), which holds so long as

$$\alpha > -\frac{r_{21}y_1^2 + r_{22}y_2^2}{s^2(r_{11}y_1^2 + r_{12}y_2^2)} \tag{33}$$

Once again we have a condition on α implying that the system will change once it becomes sufficiently negative (related to the buckling load), but that condition is expressed in terms of unknown functions.

3.3 Single-Mode Approximation

Ignoring y_2 terms, (30) becomes

$$\ddot{y} + 2\beta\dot{y} + \eta\dot{y}^2 + \omega^2 y + \gamma y^3 = p\Omega^2 \sin\Omega t \tag{34}$$

with

$$\begin{aligned}
\beta &= \frac{c_b + c_{m1}r_{41}^2}{2(1 + r_{41}^2 m)} \\
\eta &= \frac{c_{m2}r_{41}^3}{1 + r_{41}^2 m} \\
\omega^2 &= \frac{r_{21} + s^2\alpha r_{11}}{1 + r_{41}^2 m} \\
\gamma &= \frac{s^2 r_{11}^2}{2(1 + r_{41}^2 m)} \\
p &= \frac{r_{31} + r_{41}m}{1 + r_{41}^2 m} q
\end{aligned} \tag{35}$$

Of these constants, η is the only that is always negative, because so is c_{m2}. ω^2 is positive under the condition $\alpha > -r_{21}/(s^2 r_{11})$, that is (33) without y_2 terms (giving our first potentially useful determiner of the buckling point). The denominators of these parameters is related to the mass distribution: the 1 is the mass of the beam, where the $r_{41}^2 m$ adds the effect of the point mass. η and β, then, are just the damping proportional to the mass.

Higher modes represent higher energy vibrations, so if this simplified model is to be representative of the greater system, p and Ω need to be relatively small. Otherwise, the high-energy of the system will ensure that higher-energy modes not incorporated into this single-mode approximation will become relevant to the dynamics.

In addition, the mode shape ϕ remains defined in terms of the solution to a system lacking a point mass. As such, a large value of m would likely create disagreement between (34) and (6).

4 Local Bifurcation Analysis Under Static Loading

4.1 Singular Points

Setting $p = 0$ and substituting $v = \dot{y}$ into (34), we create the system of first-order ODEs

$$\begin{aligned}
\dot{y} &= v \\
\dot{v} &= -2\beta v - \eta v^2 - \omega^2 y - \gamma y^3
\end{aligned} \tag{36}$$

Singular points arise under the condition $\dot{y} = \dot{v} = 0$, which occurs when $v = 0$ and $y = 0, \pm\sqrt{-\omega^2/\gamma}$. We operate under the following assumptions about the parameters:

$$\begin{aligned}
\beta,\ \gamma &> 0 \\
\omega^2 &\in \mathbb{R} \\
|\omega^2| &\gg \beta^2
\end{aligned} \tag{37}$$

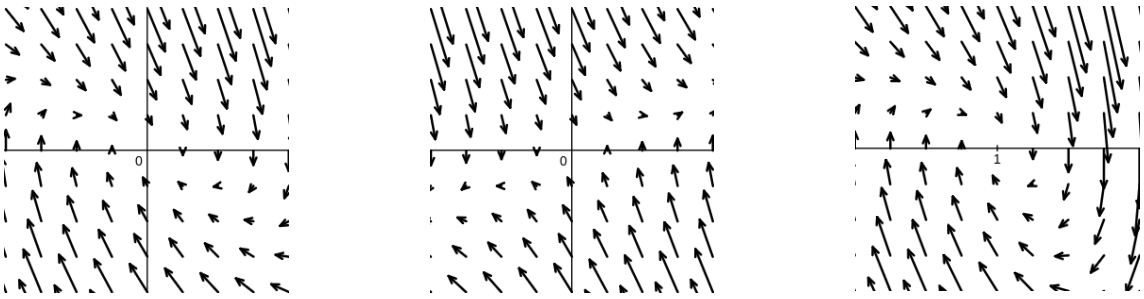

(a) $(0,0)$ for $\omega^2 = 1$ (b) $(0,0)$ for $\omega^2 = -1$ (c) $(\sqrt{-\omega^2/\gamma}, 0)$, $\omega^2 = -1$

Figure 2: orbital maps for the different singular points. The values $\beta = \gamma = 1$ were used to make these images. (a) and (c) are stable foci, (b) is a saddle.

Note that the pair of equilibria $(y, v) = (\pm\sqrt{-\omega^2/\gamma}, 0)$ are imaginary for $\omega^2 > 0$, and so can be ignored from the analysis under that condition.

The Jacobian of the system is

$$J = \begin{bmatrix} 0 & 1 \\ -\omega^2 - 3\gamma y^2 & -2\beta - 2\eta v \end{bmatrix} \tag{38}$$

A singular point is stable when the real parts of all eigenvalues of the Jacobian are negative. For the equilibrium $(y, v) = (0, 0)$, J has eigenvalues of $-\beta \pm \sqrt{\beta^2 - \omega^2}$. When $\omega^2 > 0$, the root term is imaginary so the singular point is stable, but when $\omega^2 < 0$, the relative magnitude of ω ensures that one of the eigenvalues will be positive, so the equilibrium becomes unstable. Meanwhile for the other equilibria, the eigenvalues are $-\beta \pm \sqrt{2\omega^2 + \beta^2}$. These singular points only arise as real solutions when $\omega^2 < 0$, in which case the root term is imaginary and the equilibria are stable.

4.2 Classification

The nature of the orbits around these singular points can be determined from the eigenvalues. For the stable $(0, 0)$ point, the eigenvalues are complex conjugates with negative real parts, making the point a *stable focus*. When $\omega^2 < 0$, the same singular point has one positive and one negative eigenvalue, which makes it a *saddle*. Finally, the $(y, v) = (\pm\sqrt{-\omega^2/\gamma}, 0)$ equilibria also have complex conjugate eigenvalues, making them both *stable focuses*. See Fig. (2)

4.3 Bifurcation Point

Bifurcations can occur at singular points for which the Jacobian has an eigenvalue with zero real part. In our case this occurs when $\omega^2 = 0$, for which all three singular points coincide at $(y, v) = (0, 0)$ Increasing ω^2 from this point results in one stable singular point, whereas decreasing results in two stable and one unstable, as depicted in Fig. (3). This type of bifurcation is called a *supercritical pitchfork*.

5 Analysis of the System Under Dynamic Loading

5.1 Primary Parametric Resonance

To begin to analyze (34) functionally, we assume a Multiple Scales solution of the form

$$\begin{gathered} y(t) = y_0(T_0, T_1) + \varepsilon y_1(T_0, T_1) + O(\varepsilon^2) \\ T_0 = t, \quad T_1 = \varepsilon T_0 \end{gathered} \tag{39}$$

where $\varepsilon \ll 1$ is an indicator of relative magnitude. We assume for this analysis that the parameters β, η, γ, and p are all of order ε. In addition, because we have introduced new variables, we must

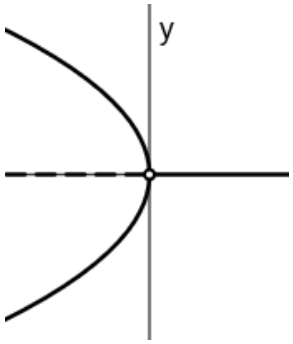

Figure 3: Bifurcation diagram on a (ω^2, y)-plane. Solid lines indicate stable equilibria whereas dashed lines are unstable.

redefine the differential operators through the chain rule:

$$\begin{aligned} \frac{d}{dt} &= D_0 + \varepsilon D_1 \\ \frac{d^2}{dt^2} &= D_0^2 + 2\varepsilon D_0 D_1 + O(\varepsilon^2) \\ D_i^j &= \frac{\partial^j}{\partial T_i^j} \end{aligned} \tag{40}$$

Applying these conditions to (34) and organizing by the order of ε gives

$$\begin{aligned} &\varepsilon^0 \left(D_0^2 y_0 + \omega^2 y_0\right) \\ &+\varepsilon^1 \left(D_0^2 y_1 + \omega^2 y_1 + 2D_0 D_1 y_0 + 2\beta D_0 y_0 + \eta (D_0 y_0)^2 + \gamma y_0^3 - p\Omega^2 \sin \Omega t\right) \\ &+O(\varepsilon^2) = 0 \end{aligned} \tag{41}$$

In order for this equality to hold, each of the magnitudes must separately equal 0. The ε^0 term is relatively straightforward:

$$y_0(T_0, T_1) = A(T_1) e^{i\omega T_0} + A^*(T_1) e^{-i\omega T_0} \tag{42}$$

where A is a complex number with conjugate A^*. Plugging this into the ε^1 term yields

$$\begin{aligned} D_0^2 y_1 + \omega^2 y_1 = &-\tfrac{1}{2} ip\Omega^2 e^{i\Omega t} - 2iA'\omega e^{i\omega T_0} - 2i\beta A\omega e^{i\omega T_0} \\ &- \eta\omega^2 (AA^* - A^2 e^{2i\omega T_0}) - \gamma (A^3 e^{3i\omega T_0} + 3A^2 A^* e^{i\omega T_0}) + cc \end{aligned} \tag{43}$$

where $A' = \frac{d}{dT_1} A$ and the cc indicates the complex conjugates of the preceding terms. To that end, the sine function of (34) was broken into complex exponentials: $\sin x = -\frac{1}{2} ie^{ix} + cc$.

To properly analyze this system near resonance ($\Omega \approx \omega$), we introduce a *detuning parameter* σ where the driving frequency $\Omega = \omega(1 + \varepsilon\sigma)$. Note that this makes $\Omega T_0 = \omega(T_0 + \sigma T_1)$. Inserting this into the (43) and collecting terms of similar frequency gives

$$\begin{aligned} D_0^2 y_1 + \omega^2 y_1 = &-\eta\omega^2 AA^* - \left(\tfrac{1}{2} ip\Omega^2 e^{i\sigma\omega T_1} + 2iA'\omega + 2i\beta A\omega + 3\gamma A^2 A^*\right) e^{i\omega T_0} \\ &+ \eta\omega^2 A^2 e^{2i\omega T_0} - \gamma A^3 e^{3i\omega T_0} + cc \end{aligned} \tag{44}$$

Meanwhile, note in general that the particular solution to an ODE of the form $\ddot{u} + \alpha^2 u = e^{i\gamma t}$ is $u = e^{i\gamma t}/(\alpha^2 - \gamma^2)$. This becomes undefined when $\alpha = \gamma$, and so these so-called *secular terms* must be removed. This is achieved by setting the coefficient of the secular term to 0. In our case, this creates the following *solvability condition*

$$\tfrac{1}{2} ip\Omega^2 e^{i\sigma\omega T_1} + 2iA'\omega + 2i\beta A\omega + 3\gamma A^2 A^* = 0 \tag{45}$$

To get useful information out of this condition, we rewrite A in polar exponential form $A = \frac{1}{2}ae^{i\psi}$. Inserting this into (45) and multiplying by $e^{-i\psi}$ gives

$$\tfrac{1}{2}ip\Omega^2 e^{i(\sigma\omega T_1 - \psi)} + i(ai\psi' + a')\omega + i\beta a\omega + \tfrac{3}{8}\gamma a^3 = 0 \tag{46}$$

Expanding out the exponential using Euler's Formula and grouping together complex and real components gives

$$\begin{aligned} \tfrac{1}{2}p\Omega^2 \sin(\sigma\omega T_1 - \psi) &= \tfrac{3}{8}\gamma a^3 - a\psi'\omega \\ \tfrac{1}{2}p\Omega^2 \cos(\sigma\omega T_1 - \psi) &= -(a' + \beta a)\omega \end{aligned} \tag{47}$$

Unfortunately, these equations state that the solvability parameters change with respect to the slow time T_1 according to yet another nonlinear differential equation. Fortunately however, if we can express this as an autonomous system of equations, we can solve for the steady state solution. To do this, we introduce another variable $\varphi = \sigma\omega T_1 - \psi$ and set $a' = \varphi' = 0$, which gives

$$\begin{aligned} \tfrac{1}{2}p\Omega^2 \sin\varphi &= \tfrac{3}{8}\gamma a^3 - a\omega^2\sigma \\ \tfrac{1}{2}p\Omega^2 \cos\varphi &= -\beta a\omega \end{aligned} \tag{48}$$

from which values for a and φ can be determined, though this particular system of equations is too elaborate to be solved algebraically. The relationship between a and σ is plotted in Fig. (4)

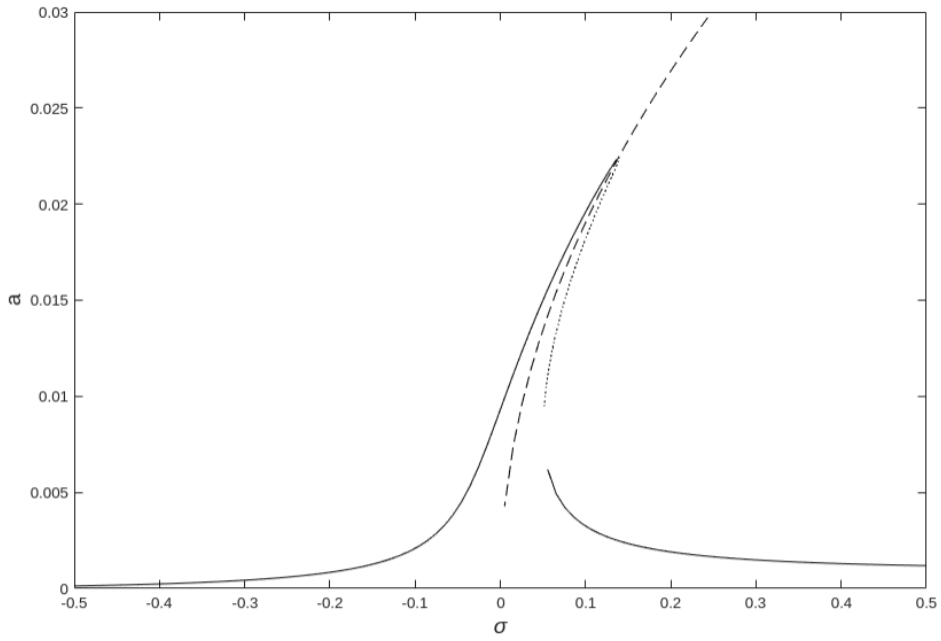

Figure 4: Stationary oscillation amplitude as a function of the detuning parameter σ, where $\sigma = 0$ corresponds to $\Omega = \omega$. The dashed line is the "backbone," corresponding to p=0. Parameter values used: $\omega^2 = 17268$, $p = 5.28 \cdot 10^{-4}$, $\beta = 2$, $\gamma = 1.27 \cdot 10^7$. The dotted line is an unstable solution to (48).

With the factor A determined, we can now solve (44) as

$$\begin{aligned} y_1 &= -\eta AA^* - \tfrac{1}{3}\eta A^2 e^{2i\omega T_0} + \frac{1}{8\omega^2}\gamma A^3 e^{3i\omega T_0} + cc \\ &= -\tfrac{1}{6}\eta a^2 \left(3 + \cos(2(\omega T_0 + \psi))\right) + \gamma\frac{a^3}{32\omega^2}\cos(3(\omega T_0 + \psi)) \end{aligned} \tag{49}$$

Noting that $\omega T_0 + \psi = \Omega t - \varphi$, then adding the y_0 term, we find

$$y(t) = a\cos(\Omega t - \varphi) - \tfrac{1}{6}\eta a^2 \left(3 + \cos(2(\Omega t - \varphi))\right) + \gamma\frac{a^3}{32\omega^2}\cos(3(\Omega t - \varphi)) \tag{50}$$

5.2 High-Frequency Response

We now use the Method of Direct Separation of Motions to examine the effects of high-frequency loading on (34).

We assume a solution of the form

$$y(t) = z(t) + \Omega^{-1}\phi(t,\tau) \tag{51}$$

subject to the restriction

$$\langle\phi\rangle \equiv \frac{1}{2\pi}\int_0^{2\pi} \phi(t,\tau)d\tau = 0 \tag{52}$$

where $\Omega^{-1} = O(\varepsilon)$ and $p\Omega = O(1)$. This setup corresponds to a slow response $z(t)$ perturbed on a fast time-scale $\tau = \Omega t$. The integral constraint ensures that the perturbation ϕ doesn't affect the value of z on the slow time-scale.

Inserting this new formulation of y into (34) gives

$$\begin{aligned}\ddot{z} + \Omega^{-1}\ddot{\phi} + 2\dot{\phi}' + \Omega\phi'' + 2\beta(\dot{z} + \Omega^{-1}\dot{\phi} + \phi') + \eta(\dot{z} + \Omega^{-1}\dot{\phi} + \phi')^2 \\ + \omega^2(z + \Omega^{-1}\phi) + \gamma(z + \Omega^{-1}\phi)^3 = p\Omega^2\sin\tau\end{aligned} \tag{53}$$

where $(\dot{}) = \frac{d}{dt}$ and $()' = \frac{d}{d\tau}$. Rearranging for ϕ'' gives

$$\phi'' = p\Omega\sin\tau - \Omega^{-1}\left(\ddot{z} + 2\dot{\phi}' + 2\beta(\dot{z} + \phi') + \eta(\dot{z} + \phi')^2 + \omega^2 z + \gamma z^3\right) + O(\Omega^{-2}) \tag{54}$$

Assuming a first-order approximation is suitable, we can simply solve this as $\phi = -p\Omega\sin\tau + O(\Omega^{-1})$.

The trick to solving for $z(t)$ is to take a fast-time average of (53); the constraint on ϕ ensures that the majority of its terms will vanish. For instance, $\langle\phi\rangle = \langle\dot{\phi}\rangle = \langle\phi'\rangle = \langle\phi''\rangle = 0$. However, $\langle\phi^2\rangle = \frac{1}{2}(p\Omega)^2$.

The result is

$$\ddot{z} + 2\beta\dot{z} + \eta\left(\dot{z}^2 + \tfrac{1}{2}(p\Omega)^2\right) + \omega^2 z + \gamma z^3 + O(\Omega^{-1}) = 0 \tag{55}$$

The form of this equation is very similar to (34), except that the harmonic forcing term is replaced by a constant proportional to η. The implication of this constant forcing is that y can oscillate around an equilibrium other than $y = 0$. This unintuitive conclusion was corroborated using the simulation tools developed in the next section, see Fig. (5).

6 Numerical Analysis

6.1 Transient Response

By breaking (34) into a pair of coupled first-order ODEs in much the same way as in section (4.1), it is easy to simulate the system using MATLAB's `ode45` function. Figures (6) and (7) show the results of these simulations for positive and negative ω^2.

These plots align with the location and nature of the singular point orbit diagrams shown in Fig. (2). When ω^2 is positive, the system spirals towards the origin, but when ω^2 is negative, the origin becomes unstable and the attractor point moves to a point along the y-axis.

6.2 Amplitude Determination

From the transient response data we can safely assume that (within the range of reasonable initial conditions) steady state operation is in affect for $t > 3$. Combining that condition with the function `islocalmax` makes it very easy to identify the response amplitude. By running a series of simulations over many forcing frequencies and at both low and high initial amplitude, two different paths through the resonance peak appear, as shown in Fig. (8).

Although this is certainly very similar to Fig. (4), it appears that the simulation is struggling to reach the peak of the curve.

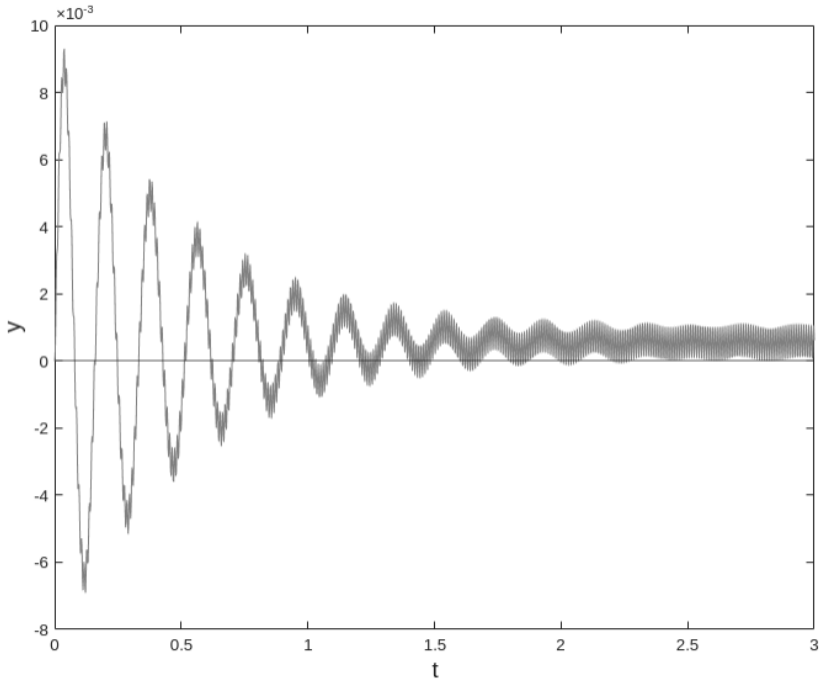

Figure 5: Simulation results of (34) for $\Omega = 20\omega$. The equilibrium is noticeably above $y = 0$.

7 Conclusion

Based on the information in the course exercise document, it appears that the motive behind all this analysis is the observation in free-response experiments of a change in oscillation frequency as the beam's vibrations decay. Linear systems have clear, well-defined resonances, but as we can see in Figures (4) and (8), that no longer holds true when nonlinearities are added: one driving frequency may result in two different response amplitudes depending on the initial conditions. Such plots are created with oscillating forcing functions at variable frequency and constant amplitude, but it stands to reason that in a free response, the decreasing amplitude would similarly cause the system to move along that curved path, which would correspond to a change in oscillation frequency.

The curved amplitude response of Fig. (4) is typical of nonlinear systems with hardening restoring forces, and in this system γ comes from the integral tension term, not the point mass. As such, it is likely that similar decay data would be observed for any tensioned beam, and the effect of the point-mass, especially the potential effects of its rotational inertia, appear to be secondary factors in the creation of the observed nonlinear behavior.

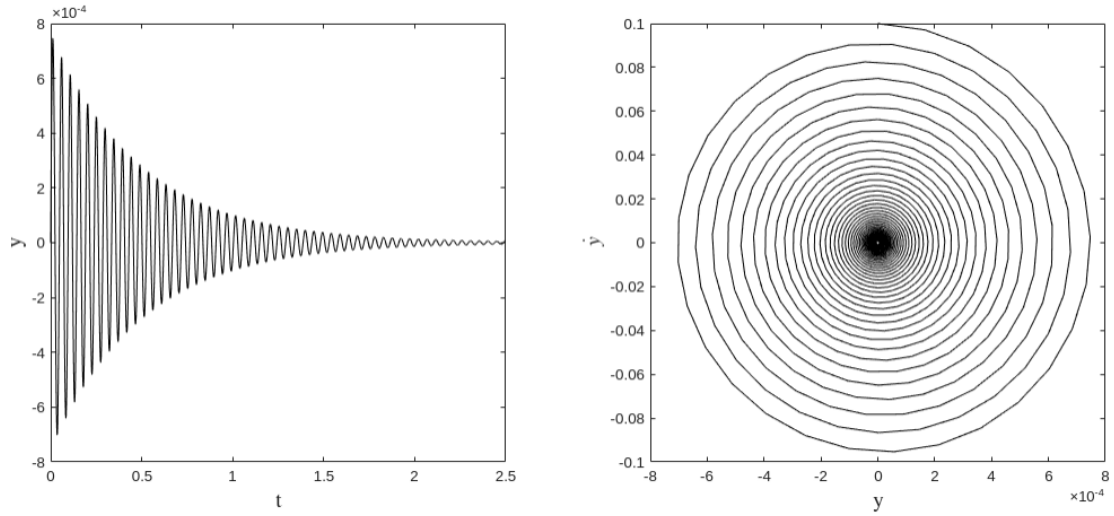

Figure 6: Transient response for $y(0) = 0$, $\dot{y}(0) = 0.1$. Parameters are the same as given in Fig. (4)

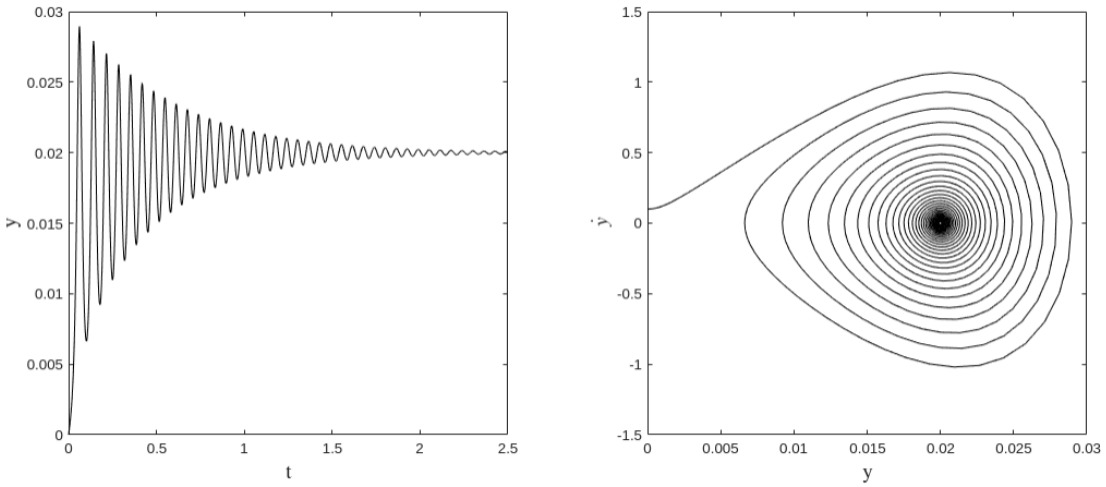

Figure 7: Transient response for $y(0) = 0$, $\dot{y}(0) = 0.1$, $\omega^2 = -5080$

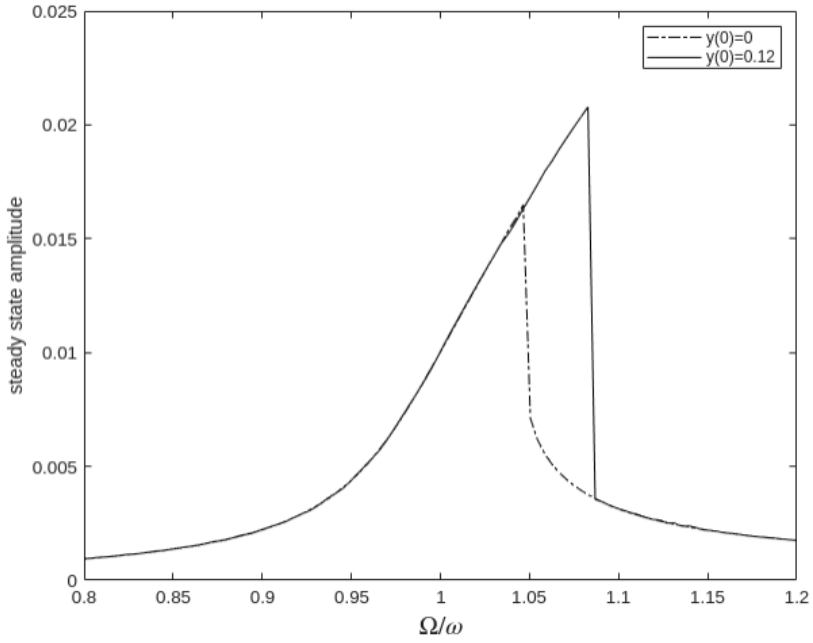

Figure 8: Stationary response over a range of driving frequencies